Dielectrophoresis-Based Cell Separation and Controlled Transportation in a Microfluidics System

Shaharia Gazi[1], A K M Shoriful Islam[2], Md. Mansur Islam[3], Israt Jahan Lamia[3], Monoara Moni[4], Omar faruk Sajid[4] Sadia Elin Khan[5], Mowazzamm Hossain Rahad[6] and Ashik Alam Sunny [6]
[1,3,6]Department of Computer Science & Mathematics, Bangladesh Agricultural University
Mymensingh, 2202, Bangladesh
[2,5]Department of Electrical & Electronic Engineering, Mymensingh Engineering College
Mymensingh, 2202, Bangladesh
[4]Department of Physics University of Chittagong,
Chittagong, 4331, Bangladesh
Email: [1]shorifulislamsimul@gmail.com, [2]hanjalarahmanmunna1772@gmail.com, [3]fahimanishe701@gmail.com,
[4]farjana.phy.116@gmail.com, [5]syedmehedi1132@gmail.com, [6]mustagis@bau.edu.bd

***Abstract*—Dielectrophoresis (DEP) is an effective mechanism for the manipulation and transportation of cells based on their dielectric properties under the conditions of a non-uniform electric field. In this paper, the DEP behavior of cancer (Lymphoma, Leukemia)cells as well as the cells of the polystyrene(PS)beads, is being studied under a microfluidics system with 30 μm spaced nine electrodes. Using COMSOL Multiphysics, I designed the model and calculated the DEP force to find the impact of the positive DEP (pDEP) on the cancer cell as well as the cell of the PS beads with the negative DEP(nDP) for their separation and transportation**

***Index Terms*—component, formatting, style, styling, insert**

I. Introduction

To investigate the effects of positive and negative dielectrophoresis (pDEP/nDEP) on polystyrene (PS) beads and cancer cells in a microfluidic system, COMSOL Multiphysics was employed. The microfluidic channel was designed with dimensions of 300 μm in length, 100 μm in width, and 50 μm in height. It contained nine electrodes, each having a width of 10 μm, a depth of 1 μm, and a height of 45 μm. Patterns of the electric field, voltage gradient, and dielectrophoretic (DEP) force were analyzed to evaluate the behavior of cells under an applied DC voltage. Cancer cells experienced pDEP forces, attracting them toward high-field regions near the electrodes, whereas PS beads were subjected to nDEP forces, moving toward low-field regions and experiencing additional lateral forces induced by the applied voltage. To ensure accurate DEP force prediction, a mathematical model was developed, and simulations of fluid flow velocity and three-dimensional electric field distribution (arrow surface plots) were performed. The results demonstrate that DEP-based cell sorting and transport are feasible and could be applied in lab-on-a-chip technologies, cancer cell detection, and biomedical diagnostics.

II. Related works

DEP is an important microfluidic method for label-free cell separation independent of size based on the dielectric properties of cells. Despite successful demonstrations, such as the use of arc-shaped chips and diverse electrode designs for cancer cell separation, achieving high recovery and purity, there are still issues of reproducibility and scalability due to differences in cell properties, electrode design, and fluid effects.

Farasat et al. provide a comprehensive review of signal-based dielectrophoresis (DEP) methods, emphasizing the role of AC field parameters, such as frequency, amplitude, phase, and waveform, in allowing label-free cell and particle separation [1]. The authors discuss advanced techniques, including multi-frequency DEP, pulsed DEP, travelling-wave DEP, and field-flow fractionation DEP, which allow for highly selective manipulation of bioparticles based on their dielectric properties. While their review focuses on complex AC-driven systems capable of multi-type cell separation, our study adopts a simpler DC-based DEP approach to demonstrate fundamental pDEP and nDEP behavior for cancer cells and polystyrene beads. This foundational work aligns with the broader goal of leveraging DEP for microfluidic cell sorting while highlighting the trade-off between simplicity and operational flexibility in DEP system design.

In a more advanced approach to DEP-based separation, Sharbati et al. proposed a microfluidic device featuring 3D electrodes capable of separating multiple cell types, including RBCs, T cells, U937-MC cells, and bacteria, in a sequential manner using frequency-dependent dielectrophoresis [2]. Their design achieved a separation efficiency of up to 95.5% while maintaining cell viability below electroporation thresholds. Unlike their tunable AC-based method, our study employs a simpler DC-driven planar electrode array to demonstrate fundamental pDEP and nDEP behavior for cancer cells and polystyrene beads, providing a foundational model that may be extended toward more complex multistage systems such as the one presented by the authors.

III. Methodology

Dielectrophoresis (DEP) is the movement of a particle in a nonuniform electric field due to the interaction between

the particle's induced dipole and the spatial gradient of the electric field. DEP provides a subtle yet effective means to manipulate particles and cells at the microscale, owing to its favorable scaling with system miniaturization. It has been widely utilized in microfluidic applications [3]. When a particle is polarized, its induced dipole moment interacts with a nonuniform electric field to generate a dielectrophoretic (DEP) force. The magnitude and direction of this force depend on both the applied electric field and the permittivity of the medium and the particle [4].

In this work, a system with nine electrodes was designed. The even-numbered electrodes were grounded at 0 V, while the odd-numbered electrodes were biased with a 10 V DC potential. The applied 10 V on the odd electrodes was time-varying, generating sinusoidal or square-wave signals, implying that AC voltage components may also exist within the microchannel layer. Consequently, a small AC component could propagate through the electrodes and microfluidic layer. Phosphate-buffered saline (PBS) was used as the suspending medium, which is commonly applied in DEP studies. Any AC voltage generated, however, is considered negligible due to the absence of significant AC noise or interference. Therefore, the F_{DEP} calculations are performed under DC voltage conditions.

An additional consideration is that PBS exhibits a conductivity of 1.5 S/m at a room temperature (25°C). For effective DEP manipulation of cancer cells and PS beads, the conductivity was reduced to 0.1 S/m. This was achieved by diluting PBS with deionized water and adjusting the ionic concentration using NaCl, KCl, Na_2HPO_4, and KH_2PO_4. The dielectrophoretic force F_{DEP} acting on the cells was then calculated. A positive F_{DEP} corresponds to positive DEP (pDEP), in which the cells are attracted toward regions of high electric field intensity. Conversely, a negative F_{DEP} indicates negative DEP (nDEP), where the cells migrate toward low-field regions.

The dielectrophoretic force can be expressed as:

$$F_{\text{DEP}} = 2\pi r^3 \varepsilon_m \left(\frac{\sigma_\rho - \sigma_m}{\sigma_\rho + 2\sigma_m} \right) \nabla |E|^2 \tag{1}$$

where:

- r = radius of the cell,
- ε_m = permittivity of PBS medium,
- σ_ρ = conductivity of the cell,
- σ_m = conductivity of the PBS,
- $\nabla |E|^2$ = gradient of the squared electric field.

The permittivity of the PBS medium is calculated as:

$$\varepsilon_m = \varepsilon_r \cdot \varepsilon_0 \tag{2}$$

where ε_r is the relative permittivity of PBS and ε_0 is the permittivity of free space.

For PBS,

$$\varepsilon_m = 80 \times 8.854 \times 10^{-12} = 7.0832 \times 10^{-10}\,\text{F/m}.$$

The gradient of the squared electric field is calculated as follows:

$$E = \frac{V}{d}, \quad V = 10\,\text{V}, \quad d = 30 \times 10^{-6}\,\text{m}$$

$$E = 3.33 \times 10^5\,\text{V/m}$$

$$|E|^2 = (3.33 \times 10^5)^2 = 1.11 \times 10^{11}$$

$$\nabla |E|^2 = \frac{3.33 \times 10^5 - 0}{30 \times 10^{-6}} = 3.7 \times 10^{15}\,\text{V}^2/\text{m}^3$$

1) For Cancer Cell:

$$\begin{aligned} F_{\text{DEP}} &= 2\pi (4 \times 10^{-6})^3 \times (7.0832 \times 10^{-10}) \\ &\quad \times \left(\frac{0.5 - 0.1}{0.5 + 20.1} \right) (3.7 \times 10^{15}) \\ &\approx 6 \times 10^{-10}\,\text{N} \end{aligned} \tag{3}$$

2) For Polystyrene (PS) Bead Cell:

$$\begin{aligned} F_{\text{DEP}} &= 2\pi (4 \times 10^{-6})^3 \times (7.0832 \times 10^{-10}) \\ &\quad \times \left(\frac{1 \times 10^{-14} - 0.1}{1 \times 10^{14} + 20.1} \right) (3.7 \times 10^{15}) \\ &\approx -5.3 \times 10^{-10}\,\text{N} \end{aligned} \tag{4}$$

A. Model Setup

In this model, two cells are positioned approximately 210 μm apart to ensure that the DEP forces are correctly calculated without mutual interference. A cancer cell is placed near the laminar flow (SPF) inlet wall along the electrode, while the PS bead is positioned on the opposite corner near the outlet flow wall.

An upper layer of polydimethylsiloxane (PDMS) of thickness 1 μm is added, ensuring no interference with the electric field in the microfluidic channel (PBS). The electrode dimensions are:

- Depth (thickness): 1 μm
- Width: 10 μm
- Height: 45 μm
- Total number of electrodes: 9

The radius of both cells was taken as 4 μm to ensure accurate results.

Also, I calculated the DEP force components (F_x, F_y, F_z) concerning cancer cells and PS beads, based on $\text{Re}[k(\omega)]$, the real part of the Clausius–Mossotti factor.

The time-averaged dielectrophoretic (DEP) force $\vec{F}_{\text{DEP}}$ of a spherical particle is given by:

$$\vec{F}_{\text{DEP}} = 2\pi r^3 \varepsilon_m \,\text{Re}[k(\omega)]\, \nabla |\vec{E}_{\text{rms}}|^2 \tag{5}$$

where the Clausius–Mossotti factor is defined as:

$$\text{Re}[k(\omega)] = \text{Re}\left(\frac{\varepsilon_p - \varepsilon_m}{\varepsilon_p + 2\varepsilon_m} \right) \tag{6}$$

Here,

- ε_p = complex permittivity of the particle (cancer cell / PS bead),

- ε_m = complex permittivity of the medium.

After calculation, we obtain:

$\mathrm{Re}[k(\omega)] = 0.571$ for cancer cells, $\mathrm{Re}[k(\omega)] = -0.5$for PS bea

The DEP force components (F_x, F_y, F_z) were then calculated using (5) and the values of $\mathrm{Re}[k(\omega)]$ for both types of particles.

1) For Cancer Cell: $F_x = -1.48 \times 10^{-10}$N, $F_y = -6.97 \times 10^{-11}$ N, $F_z = -3.10 \times 10^{-11}$ N

2) For PS Bead Cell: $F_x = 1.30 \times 10^{-10}$ N, $F_y = 6.11 \times 10^{-11}$ N, $F_z = 2.713 \times 10^{-11}$ N

B. Reynolds Number (R_e) Calculation

The Reynolds number is defined as the ratio of inertial force to viscous force:

$$R_e = \frac{\rho V D}{\mu} \tag{7}$$

where

- ρ = density of the fluid,
- V = velocity of the flow,
- D = hydraulic diameter of the rectangular channel,
- μ = dynamic viscosity of the fluid.

The hydraulic diameter D for a rectangular channel is given by:

$$D = \frac{2hw}{h + w} \tag{8}$$

Substituting the channel dimensions:

$$D = \frac{2 \times (50 \times 10^{-6})(100 \times 10^{-6})}{50 \times 10^{-6} + 100 \times 10^{-6}} = 66.7 \times 10^{-6}\,\mathrm{m}$$

$$R_e = \frac{1000 \times (7 \times 10^{-4}) \times (66.7 \times 10^{-6})}{0.89 \times 10^{-3}} \tag{9}$$

$$R_e \approx 0.05246$$

IV. SIMULATION MODEL

In this model, two cells are positioned approximately 210 μm apart to ensure that the DEP force is calculated correctly without mutual interference. A cancer cell is placed near the laminar flow (SPF) inlet wall along the electrode, while the PS bead cell is located at the opposite corner near the outlet flow wall.

An upper layer of polydimethylsiloxane (PDMS) of thickness 1 μm is included, which does not interfere with the electric field within the microfluidic channel (PBS). The electrodes are designed with the following dimensions:

- Depth (thickness): 1 μm
- Width: 10 μm
- Height: 45 μm
- Total number of electrodes: 9

The radius of both cells was taken as 4 μm to obtain accurate simulation results.

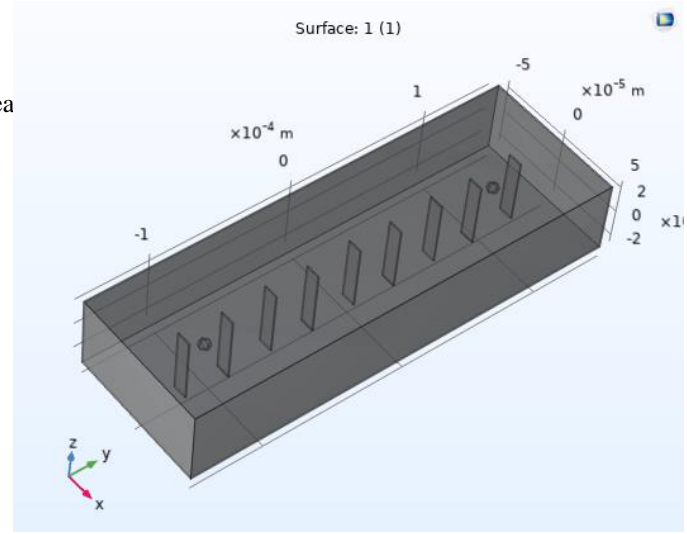

Fig. 1. 3D simulation model

V. RESULTS & FINDINGS

Theoretical and mathematical analysis confirmed that the dielectrophoretic force (F_{DEP}) differs significantly between the two cell types. For cancer cells, F_{DEP} was 6×10^{-10} N, corresponding to positive DEP (pDEP) that drives the cells toward high electric field regions near electrodes. In contrast, PS beads exhibited $F_{\mathrm{DEP}} = -5.3 \times 10^{-10}$ N, showing negative DEP (nDEP), which pushes them away from electrode edges toward low-field regions at the channel center. These opposite responses form the basis of the controlled separation.

Figure 2 presents the electric field distribution (EFD). The field intensity peaks near electrode edges, creating localized "hot spots" that generate strong DEP forces. These regions are responsible for attracting cancer cells by pDEP and repelling PS beads by nDEP. Medium-strength regions around the electrodes support additional manipulation, while weaker fields at the channel center contribute minimally.

Figures 3–4 illustrate the DEP component forces. For cancer cells, arrows point toward the electrodes, confirming pDEP-driven trapping. For PS beads, arrows are directed away from the electrodes, verifying nDEP migration. Since $\mathrm{Re}[K(\omega)] > 0$ for cancer cells and $\mathrm{Re}[K(\omega)] < 0$ for PS beads, the theoretical calculations are directly validated.

A. DEP and Flow Interaction

The velocity profile of the microchannel (Fig. 5) shows higher velocities at the channel center and reduced flow near electrode walls. This flow pattern plays a complementary role in DEP manipulation. Cancer cells undergoing pDEP migrate to electrode regions, where velocity is low, allowing them to remain trapped. In contrast, PS beads experiencing nDEP are directed to the center, where fluid velocity is highest, ensuring faster downstream transport.

Streamline analysis (Fig. 6) further emphasizes this behavior. Field lines converge strongly near electrode edges, attracting the more polarizable cancer cells (pDEP). Conversely, the

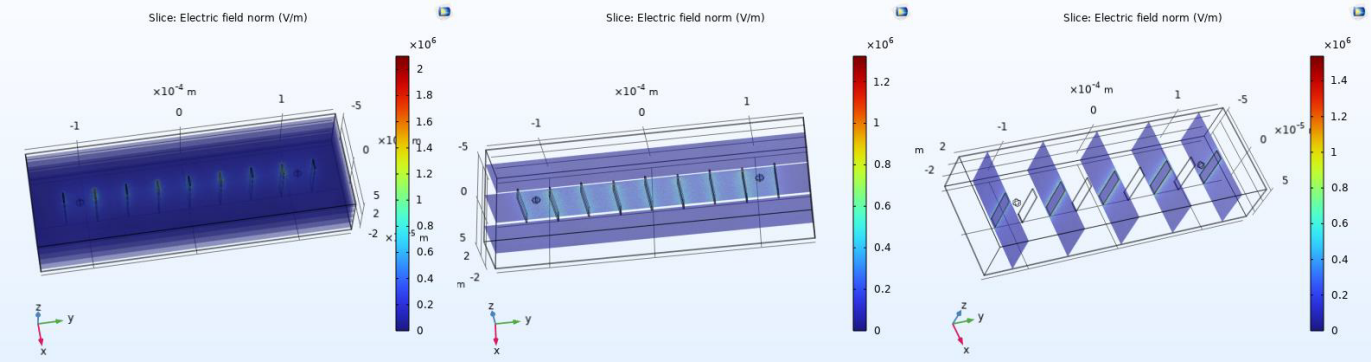

Fig. 2. Electric field norm (V/m) on the xy, yz, and zx axes, showing strong gradients at electrode edges.

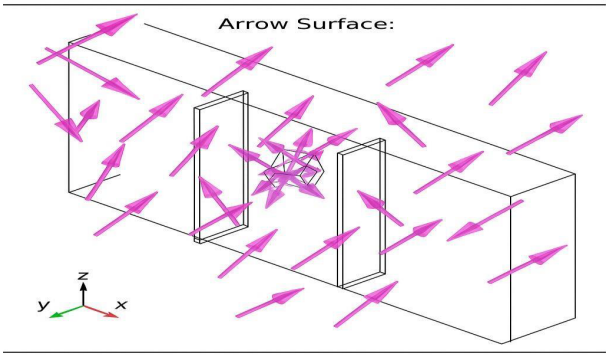

Fig. 3. DEP component forces (F_x, F_y, F_z) acting on a cancer cell ($\mathrm{Re}[K(\omega)] > 0$).

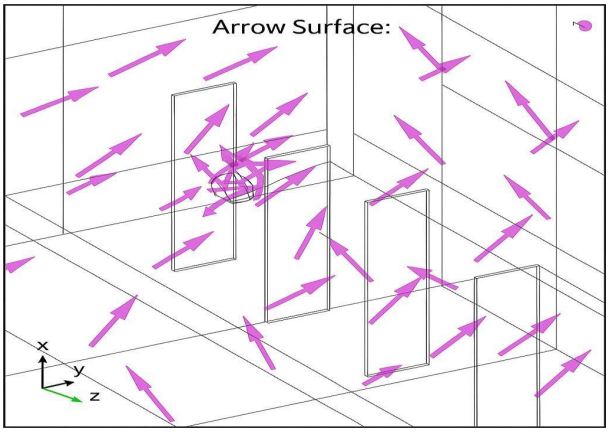

Fig. 4. DEP forces on PS bead cell, showing nDEP away from electrodes toward channel center.

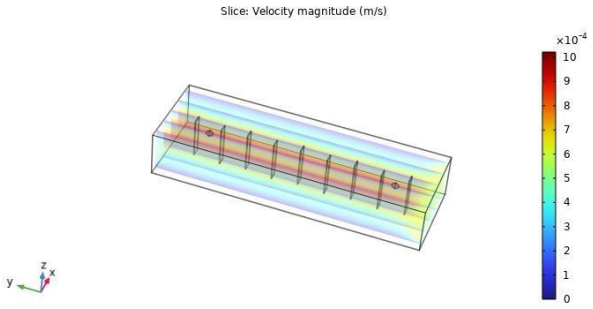

Fig. 5. Fluid velocity distribution (m/s) in the microchannel.

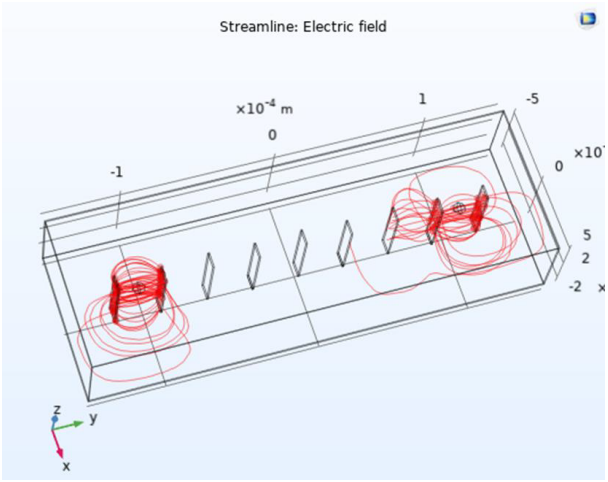

Fig. 6. Streamline analysis of electric field distribution.

less polarizable PS beads are repelled to the center, aligning with high-velocity streamlines. This confirms simultaneous trapping of cancer cells and rapid transport of PS beads.

B. DEP Force Distribution

Arrow volume plots (Fig. 7) show localized strong vectors at electrode edges (responsible for pDEP) and weaker vectors pointing toward the center (driving nDEP). This spatial distribution confirms the controlled separation: cancer cells remain confined near electrodes, while PS beads migrate centrally under combined nDEP and hydrodynamic drag.

Contour plots quantify these regions: 2.46×10^5–1.23×10^6 V/m near electrodes (pDEP) versus 8.2×10^4–7.38×10^5 V/m at the channel center (nDEP). Arrow surface plots (Fig. 8) highlight dense vectors at electrodes, further confirming hotspot-driven DEP forces.

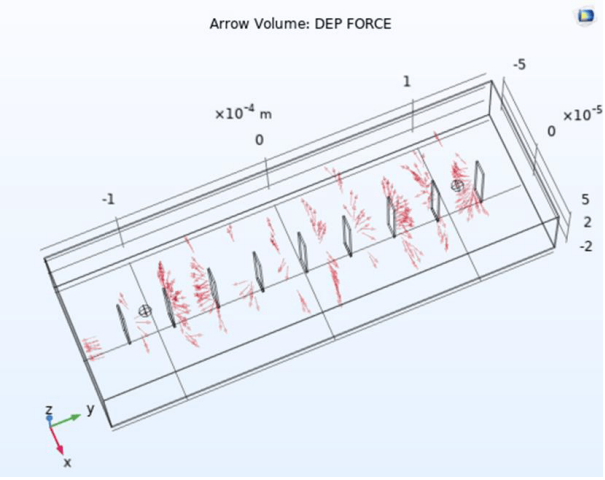

Fig. 7. DEP force distribution along the microchannel.

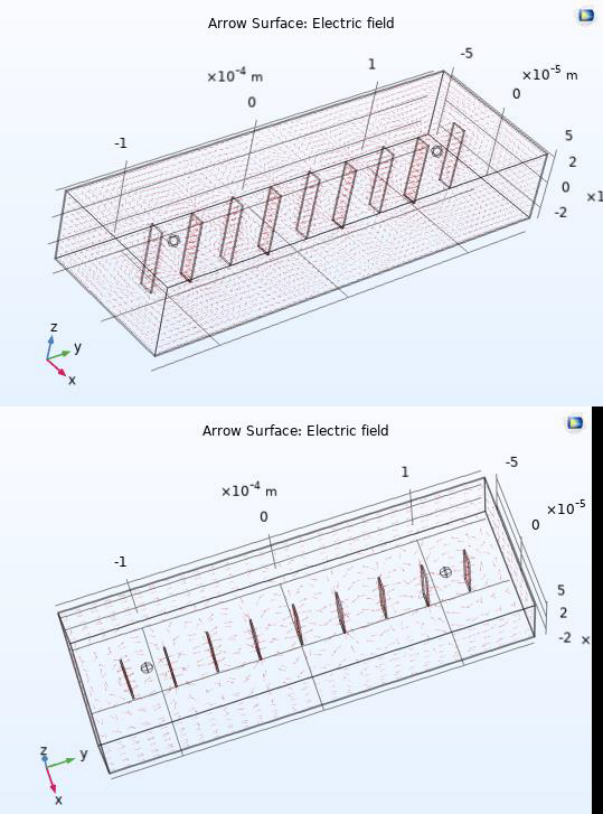

Fig. 8. Electric field vector surface plot showing concentration near electrodes.

C. Reynolds Number Justification

The calculated Reynolds number is $Re \approx 0.052$, which is well within the laminar regime ($Re < 1$). Such smooth, predictable flow ensures precise control of particle trajectories and prevents turbulence that could disrupt DEP-based separation.

D. Novelty

The proposed design achieves label-free separation of cancer and PS cells under low Reynolds number flow. Unlike conventional approaches relying on biomarkers or high flow rates, the novel electrode arrangement produces a non-uniform field that amplifies DEP sensitivity. Placing cells symmetrically in the channel enables direct comparison of differential responses in real time. By integrating electric field distribution, fluid dynamics, and particle motion, this model provides a realistic and cost-effective platform for early cancer diagnostics using DEP-based microfluidics.

VI. Conclusion

In this paper, using dielectrophoresis (DEP), we illustrated the controlled transport of two different cells: cancer cell & polystyrene (PS) bead cell within a microchannel containing microfluidics diluted phosphate-buffered saline(PBS). By simulating and doing the mathematical calculation, we justified that the cancer cell gets positive dielectrophoresis (pDEP) and is attracted towards the dense electric field area closer to the electrodes. On the contrary, the polystyrene (PS) bead cell shows negative dielectrophoresis (nDEP) characteristics which caused its transportation towards the center of the channel. This argument was derived through multiple ways such as DEP force mathematical calculations also electric field distribution plots, arrow surface plots, and velocity plots. Velocity plot helps to understand the transportation of both cells along with the fluid motion. The velocity profile goes under the Poiseuille flow pattern which influences a vital role of transporting cells. The PS Beads cell gets repelled to the middle of the fluid channel (higher velocity of fluid) enabling hydrodynamic motion that interplay with DEP force. That creates an opportunity for microfluidic shorting techniques using DEP that is feasible and can be used in both the sector of biological and synthetic particles. This study shows a strong base for particle manipulation using DEP. Numerous features can be investigated and researched further for future aspects.

References

[1] M. Farasat, E. Aalaei, S. Kheirati Ronizi, A. Bakhshi, S. Mirhosseini, J. Zhang, N.-T. Nguyen, and N. Kashaninejad, "Signal-based methods in dielectrophoresis for cell and particle separation," *Biosensors*, vol. 12, no. 7, p. 510, 2022.

[2] P. Sharbati, A. K. Sadaghiani, and A. Koşar, "New generation dielectrophoretic-based microfluidic device for multi-type cell separation," *Biosensors*, vol. 13, no. 4, p. 418, 2023.

[3] B. Çetin and D. Li, "Dielectrophoresis in microfluidics technology," *Electrophoresis*, vol. 32, no. 18, pp. 2410–2427, 2011.

[4] H. Morgan, N. G. Green *et al.*, "Ac electrokinetics: colloids and nanoparticles," Research Studies Press, Tech. Rep., 2003.